

THE BIAS-VARIANCE TRADE-OFF IN THOMSON'S MULTITAPER ESTIMATOR

LUÍS DANIEL ABREU AND JOSÉ LUIS ROMERO

ABSTRACT. At the heart of non-parametric spectral estimation, lies the dilemma known as the *bias-variance trade-off*: low-biased estimators tend to have high variance and low variance estimators tend to have high bias. In 1982, Thomson introduced a multitaper method where this trade-off is made explicit by choosing a target bias resolution and obtaining a corresponding variance reduction. The method became the standard in many applications. Its favorable bias-variance trade-off is due to an empirical fact, conjectured by Thomson based on numerical evidence: assuming bandwidth W and N time domain observations, *the average of the square of the first $K = \lfloor 2NW \rfloor$ Slepian functions approaches, as K grows, an ideal band-pass kernel for the interval $[-W, W]$.* We provide an analytic proof of this fact and quantify the approximation error in the L^1 norm; the approximation error is then used to control the bias of the multitaper estimator resulting from spectral leakage. This leads to new performance bounds for the method, explicit in terms of the bandwidth W and the number N of time domain observations. Our method is flexible and can be extended to higher dimensions and different geometries.

1. INTRODUCTION

Let $I = [-1/2, 1/2]$. Any stationary, real, ergodic, zero-mean, Gaussian stochastic process has a *Cramér spectral representation*

$$x(t) = \int_I e^{2\pi i \xi t} dZ(\xi),$$

and the *spectrum* $S(\xi)$, defined as

$$S(\xi)d\xi = \mathbb{E}\{|dZ(\xi)|^2\},$$

and often called the *power spectral density* of the process, yields the periodic components of $x(t)$. The goal of spectral estimation is to solve the highly underdetermined problem of *estimating $S(\xi)$ from a sample of N contiguous observations $x(0), \dots, x(N-1)$* . Embryonic

L. D. A. was supported by the Austrian Science Fund (FWF) START-project FLAME ("Frames and Linear Operators for Acoustical Modeling and Parameter Estimation") 551-N13. J. L. R. gratefully acknowledges support from a Marie Curie fellowship, within the 7th. European Community Framework program, under grant PIFI-GA-2012-327063.

approaches to the problem (Stokes 1879, Shuster 1898) used the so called *periodogram*:

$$(1.1) \quad \widehat{S}(\xi) = \frac{1}{N} \left| \sum_{t=0}^{N-1} x(t) e^{-2\pi i \xi t} \right|^2,$$

whose analysis has influenced harmonic analysts since Norbert Wiener (see [4]). The periodogram can also be weighted with a data window $\{D_t\}_{t=0}^{N-1}$, usually called a *taper*, giving the estimator:

$$(1.2) \quad \widehat{S}_D(\xi) = \left| \sum_{t=0}^{N-1} x(t) D_t e^{-2\pi i \xi t} \right|^2.$$

The choice of the taper $\{D_t\}_{t=0}^{N-1}$ can have a significant effect on the resulting spectrum estimate \widehat{S}_D . This is apparent by observing that its expectation is the convolution of the *true (nonobservable) spectrum* $S(\xi)$ with the *spectral window* $|\mathcal{F}D(\xi)|^2 = \left| \sum_{t=0}^{N-1} D_t e^{-2\pi i \xi t} \right|^2$, i.e.,

$$(1.3) \quad \mathbb{E} \left\{ \widehat{S}_D(\xi) \right\} = S(\xi) * |\mathcal{F}D(\xi)|^2.$$

Thus, the bias of the tapered estimator, which is the difference $S(\xi) - \mathbb{E}\{\widehat{S}_D(\xi)\}$, is determined by the smoothing effect of $\{D_t\}_{t=0}^{N-1}$ over the true spectrum. Ideally, the function $\mathcal{F}D(\xi)$ should be concentrated on the interval $[-\frac{1}{2N}, \frac{1}{2N}]$, but the *uncertainty principle of Fourier analysis* precludes such perfect concentration. Inevitably, some portion of the filter $\mathcal{F}D(\xi)$ will lie outside the target region and *spectral leakage* occurs.

In [23], Thomson used the sequences which minimize spectral leakage to construct an algorithm using several tapered estimates, whence the name *multitaper*. In doing so, he was able to reduce variance by averaging, while introducing a tolerable amount of spectral leakage. Thomson's multitaper method has been used in a variety of scientific applications including climate analysis (see, for instance [5], or [9] for a local spherical approach), and it was used to better understand the relation between atmospheric CO_2 and climate change (see [24, Section 1]). The method became also paramount in statistical signal analysis [17].

Today, Thomson's multitaper method remains an effective spectral estimation method. It has recently found remarkable applications in electroencephalography [7] and it is the preferred spectral sensing procedure [8] for the rapidly emerging field of cognitive radio [10]. In the next paragraph we provide an outline of the essence of the method.

Thomson's method starts by selecting a target frequency smoothing band $[-W, W]$ with $1/2N < W < 1/2$, thus accepting a reduction in spectral resolution by a factor of about $2NW$. The *first step* consists of obtaining a number $K = \lfloor 2NW \rfloor$ (the smallest integer not greater than $2NW$) of estimates of the form (1.2) by setting, for every $k \in \{0, \dots, K-1\}$, $D_t = v_t^{(k)}(N, W)$, where the *discrete prolate spheroidal sequences* $v_t^{(k)}(N, W)$ are defined as

the solutions of the Toeplitz matrix eigenvalue equation

$$\sum_{n=0}^{N-1} \frac{\sin 2\pi W (t-n)}{\pi (t-n)} v_n^{(k)}(N, W) = \lambda_k(N, W) v_t^{(k)}(N, W).$$

The resulting tapered periodogram is then denoted by $\widehat{S}_k(\xi)$. The *second step* consists of averaging. One uses the estimator

$$(1.4) \quad \widehat{S}_{(K)}(\xi) = \frac{1}{K} \sum_{k=0}^{K-1} \widehat{S}_k(\xi),$$

which achieves a reduced variance (see [23] for an asymptotic analysis of slowly varying spectra and [25, 15] for non-asymptotic expressions).

To inspect the performance of the estimator $\widehat{S}_{(K)}(\xi)$ on the spectral domain, let us consider the *discrete prolate spheroidal functions*, also known as *Slepians*. They are the discrete Fourier transforms of the sequences $v_t^{(k)}(N, W)$, denoted by $U_k(N, W; \xi)$, and satisfy the integral equation

$$(1.5) \quad \int_{-W}^W \mathbf{D}_N(\xi - \xi') U_k(N, W; \xi') d\xi' = \lambda_k(N, W) U_k(N, W; \xi),$$

where

$$(1.6) \quad \mathbf{D}_N(x) = \frac{\sin N\pi x}{\sin \pi x}$$

is the Dirichlet kernel. Observe that, according to (1.3), $\mathbb{E}\{\widehat{S}_k(\xi)\}$ is a smoothing average of the unobservable spectrum by the kernel $|U_k(N, W; \xi)|^2$. Recall that the bias of each individual estimate in (1.4) is given by

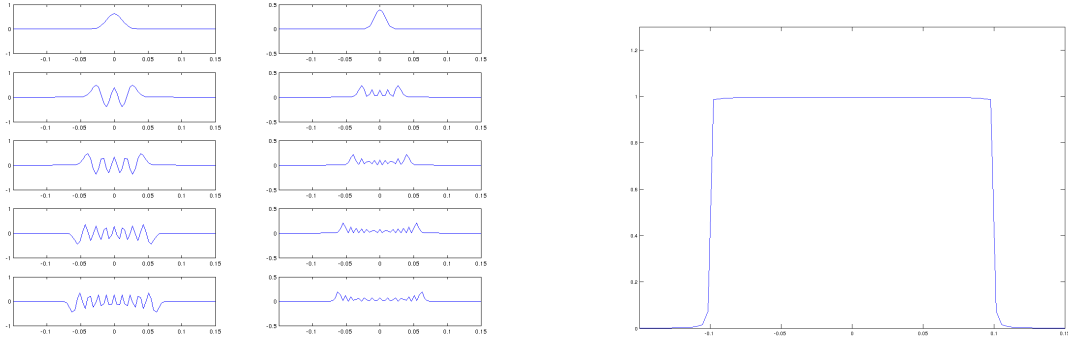
$$(1.7) \quad \text{Bias}(\widehat{S}_k(\xi)) = \mathbb{E}\{\widehat{S}_k(\xi)\} - S(\xi) = S(\xi) * |U_k(N, W; \xi)|^2 - S(\xi).$$

The optimal concentration of the first prolate function on the interval $[-W, W]$ leads to a low bias when $k = 0$. But since the amount of energy of $U_k(N, W; \xi)$ inside $[-W, W]$ decreases with k (because the energy is given by the eigenvalues in (1.5) and they decrease from 1 to 0 as k approaches K), the bias increases with k . To explain the remarkable performance of the *averaged* estimator, Thomson noted the following: the expected value of the estimator (1.4) is given by

$$(1.8) \quad \mathbb{E}\{\widehat{S}_{(K)}(\xi)\} = \frac{1}{K} \sum_{k=0}^{K-1} \mathbb{E}\{\widehat{S}_k(\xi)\} = S(\xi) * \frac{1}{K} \rho_K(N, W; \xi),$$

where

$$(1.9) \quad \frac{1}{K} \rho_K(N, W; \xi) = \frac{1}{K} \sum_{k=0}^{K-1} |U_k(N, W; \xi)|^2$$



(a) Slepian's U_k and their squares $|U_k|^2$, for $k = 1, 5, 9, 19$.

(b) Thomson's spectral window.

FIGURE 1. Some Slepian's and the spectral window with $N = 256$ and $w = 0.1$.

is the *spectral window* of (1.8). The bias performance is due to the fact, numerically illustrated by Thomson, that the spectral window (1.9) is very similar to a flat function localized on $[-W, W]$ (see Figure 1). This is an intriguing mathematical phenomenon. Heuristically, it requires the functions in the sequence $\{|U_k(N, W, \cdot)|^2 : k = 0, \dots, K-1\}$ to be organized inside the interval $[-W, W]$ in a very particular way: *each function tends to fill in the empty energy spots left by the sum of the previous ones*. This behavior is reminiscent of the Pythagorean relation for pure frequencies: $\sin^2(t) + \cos^2(t) = 1$. More precisely, claiming that the spectral window in Thomson's method approximates an ideal band-pass kernel, means that the two functions

$$(1.10) \quad \frac{1}{K} \rho_K(N, W, \cdot) \quad \text{and} \quad \frac{1}{2W} \mathbf{1}_{[-W, W]},$$

approach each other as K increases. This is indeed true and we provide an analytic bound for the L^1 -distance between the functions in (1.10).

Theorem 1 (Spectral leakage estimate). *Let $N \geq 2$ be an integer, $W \in (-1/2, 1/2)$ and set $K := \lfloor 2NW \rfloor$. Then*

$$(1.11) \quad \left\| \frac{1}{K} \rho_K(N, W, \cdot) - \frac{1}{2W} \mathbf{1}_{[-W, W]} \right\|_{L^1(I)} \lesssim \frac{\log N}{K}.$$

The spectral leakage estimate (1.11) is precisely what we need in order to quantify Thomson's asymptotic analysis of the bias of the multitaper estimator [23, pag. 1062] and validate the bias-variance trade-off. This is explained in the Conclusion section.

A relevant feature of the method introduced in this paper is its flexibility. While the description of each individual solution to the concentration problem in (1.5) is very subtle, the *aggregated behavior* of the critical number of solutions to (1.5) displays a simple profile.

A similar aggregated behavior has been investigated in [2] and numerically illustrated in [3, 6].

Our analysis depends on the properties of the eigenvalues in (1.5). Similar properties have been recognized in the eigenvalue problem in the context of Hankel bandlimited functions [1]. Since the problem studied in [1] includes the one considered by Slepian in his construction of $2d$ radial prolate functions, we expect our methodology to be applicable to spectral estimation problems involving $2d$ functions whose spectrum lies on a disk. This may have applications in cryo-electron microscopy, where estimation of noise stochastics is an important consideration when applying PCA to microscopy images [26]. Other multitaper estimators include multi-window estimators for non-stationary spectrum [3, 16] and the one based on spherical Slepian functions [19, 6].

2. PROOF OF THE MAIN RESULT

Our proof uses tools from the Landau-Pollack-Slepian theory [20, 22, 12, 13, 14]. We do not rely on special properties of the interval I , but rather on so-called trace / norm estimates that can be obtained in many other contexts of practical interest (e.g. [1]). Hence the flexibility of our approach.

Let $I := [-1/2, 1/2]$ and let us denote the exponentials by $e_\omega(x) := e^{2\pi i x \omega}$. We will always let $N \geq 2$ be an integer and $W \in (-1/2, 1/2)$. For two non-negative functions f, g , the notation $f \lesssim g$ means that there exists a constant $C > 0$ such that $f \leq Cg$. (The constant C , of course, does not depend on the parameters N, W .)

2.1. Trigonometric polynomials. For notational convenience, we use a temporal normalization that is slightly different of the one in the Introduction (this has no impact in the announced estimates). We consider the space of trigonometric polynomials

$$\mathcal{P}_N = \text{Span} \left\{ e_{-\frac{N+1}{2}+j} : 0 \leq j \leq N-1 \right\} \subseteq L^2(I).$$

This is a Hilbert space with a reproducing kernel given by the translated Dirichlet kernel, $\mathbf{D}_N(x-y)$, $x, y \in I$, $N \in \mathbb{N}$, where \mathbf{D}_N is given by (1.6). Note that $\int_I |\mathbf{D}_N|^2 = N$.

2.2. Toeplitz operators. For $W \in (-1/2, 1/2)$ the *Toeplitz operator* H_W^N is

$$(2.1) \quad H_W^N f := P_{\mathcal{P}_N} \left((P_{\mathcal{P}_N} f) \cdot 1_{[-W, W]} \right), \quad f \in L^2(I),$$

where $P_{\mathcal{P}_N}$ is the orthogonal projection onto \mathcal{P}_N . When $f \in \mathcal{P}_N$, $H_W^N f$ is simply the projection of $f \cdot 1_{[-W, W]}$ into \mathcal{P}_N . The Slepian functions $\{U_k(N, W) : k = 0, \dots, N-1\}$ are the eigenfunctions of H_W^N with corresponding eigenvalues $\lambda_k = \lambda_K(N, W)$:

$$(2.2) \quad \int_{-W}^W |U_k(N, W; \xi)|^2 d\xi = \lambda_k,$$

ordered non-increasingly. We normalize the Slepian functions by: $\int_I |U_k(N, W; \xi)|^2 d\xi = 1$. We will need a description of the profile of the eigenvalues of H_W^N .

Lemma 1. *For $N \geq 2$, $W \in (-1/2, 1/2)$ and $K := \lfloor 2NW \rfloor$:*

$$(2.3) \quad \left| 1 - \frac{1}{K} \sum_{k=0}^{K-1} \lambda_k(N, W) \right| \lesssim \frac{\log N}{K}.$$

We postpone the proof of Lemma 1 to the Appendix. The quantity on the left-hand side of (2.3) has been studied in [15] to qualitatively analyze the performance of Thomson's method. Lemma 1 refines the analysis of [15], giving a concrete growth estimate. (See also the remarks after Theorem 5 in [15].)

2.3. Proof of Theorem 1. We first estimate the narrow band error. Note that $\rho_K(N, W; \xi) = \sum_{k=0}^{K-1} |U_k(N, W; \xi)|^2 \leq \sum_{k=0}^{N-1} |U_k(N, W; \xi)|^2 = D_N(0) = N$. Consequently, $\frac{1}{K} \rho_K(N, W; \xi) \leq \frac{N}{K}$ and, using (2.2), we can estimate:

$$\begin{aligned} & \int_{-W}^W \left| \frac{1}{K} \rho_K(N, W; \xi) - \frac{1}{2W} \mathbf{1}_{[-W, W]}(\xi) \right| d\xi \\ & \leq \int_{-W}^W \left| \left(\frac{1}{2W} - \frac{N}{K} \right) \mathbf{1}_{[-W, W]}(\xi) \right| d\xi + \int_{-W}^W \left| \frac{1}{K} \rho_K(N, W; \xi) - \frac{N}{K} \mathbf{1}_{[-W, W]}(\xi) \right| d\xi \\ & = 2W \left(\frac{N}{K} - \frac{1}{2W} \right) + \frac{2NW}{K} - \frac{1}{K} \sum_{k=0}^{K-1} \int_{-W}^W |U_k(N, W; \xi)|^2 d\xi \\ & \leq \frac{2}{K} + 1 - \frac{1}{K} \sum_{k=0}^{K-1} \lambda_k \lesssim \frac{\log N}{K}, \end{aligned}$$

thanks to Lemma 1. Now we estimate the broad brand leakage:

$$\begin{aligned} & \int_{I \setminus [-W, W]} \left| \frac{1}{K} \rho_K(N, W; \xi) - \frac{1}{2W} \mathbf{1}_{[-W, W]}(\xi) \right| d\xi = \int_{I \setminus [-W, W]} \frac{1}{K} \rho_K(N, W; \xi) d\xi \\ & = \frac{1}{K} \sum_{k=0}^{K-1} (1 - \lambda_k) = 1 - \frac{1}{K} \sum_{k=0}^{K-1} \lambda_k, \end{aligned}$$

so the conclusion follows invoking again Lemma 1.

3. CONCLUSION

In [23, Section IV], Thomson estimated $\text{Bias}(\hat{S}_{(K)})$ by using the approximation $\frac{1}{K} \rho_K(N, W, \cdot) \approx \frac{1}{2W} \mathbf{1}_{[-W, W]}$. Besides supporting that reasoning, Theorem 1 allows one to quantify the bias. Indeed,

$$\left| \text{Bias}(\hat{S}_{(K)}(\xi)) \right| \leq \left\| S * \frac{1}{K} \rho_K(N, W, \cdot) - S * \frac{1}{2W} \mathbf{1}_{[-W, W]} \right\|_{\infty} + \left\| S - S * \frac{1}{2W} \mathbf{1}_{[-W, W]} \right\|_{\infty}$$

and, if S is a bounded function, then Theorem 1 implies that

$$\left\| S * \frac{1}{K} \rho_K(N, W, \cdot) - S * \frac{1}{2W} \mathbf{1}_{[-W, W]} \right\|_{\infty} \lesssim \max_{\xi' \in \mathbb{R}} |S(\xi')| \frac{\log N}{K}.$$

The remaining term $\|S - S * \frac{1}{2W} \mathbf{1}_{[-W, W]}\|_{\infty}$ can be bounded by assuming that S is smooth. For example, if, as in Thomson's work, S is assumed to be analytic (and periodic), then $\|S - S * \frac{1}{2W} \mathbf{1}_{[-W, W]}\| \lesssim W^2$, leading to the bias estimate:

$$(3.1) \quad \text{Bias}(\hat{S}_{(K)}(\xi)) \lesssim W^2 + \frac{\log N}{K}.$$

On the other hand, for a slowly varying spectrum S , Thomson [23] argues that

$$(3.2) \quad \text{Var}(\hat{S}_{(K)}(\xi)) \lesssim \frac{1}{K},$$

(see, [25], [15] or [11, Section 3.1.2] for precise expressions for the variance.) Given a number of available observations, the estimates in (3.1) and (3.2) show how much bias can be expected, in order to bring the variance down by a factor of $1/K$. This leads to a concrete estimate for the mean squared error

$$(3.3) \quad \text{MSE}(\hat{S}_{(K)}) = \mathbb{E}(S - \hat{S}_{(K)})^2 = \text{Bias}(\hat{S}_{(K)})^2 + \text{Var}(\hat{S}_{(K)}) \lesssim W^4 + \frac{\log^2 N}{K^2} + \frac{1}{K},$$

that can be used to decide on the value of the bandwidth resolution parameter W .

We have thus obtained explicit bounds that allow us to quantify the bias-variance trade-off in Thomson's multitaper method. Note that in the slowly varying regime, the error due to spectral leakage is largely dominated by the variance and therefore, in agreement with Thomson's analysis, the mean squared error is $\approx W^4 + \frac{1}{K}$. In the case of more rapidly varying spectra, (3.2) is no longer a valid approximation [25, 15] and the contribution of the spectral leakage to the mean squared error can be more significant.

4. APPENDIX

4.1. Integral kernels. The Toeplitz operator H_W^N from (2.1) can be explicitly described by the formula

$$H_W^N f(x) = \int_I f(y) K_W^N(x, y) dy,$$

where the kernel $K_W^N(x, y)$ is

$$(4.1) \quad K_W^N(x, y) = \int_{[-W, W]} \mathbf{D}_N(x - z) \overline{\mathbf{D}_N(y - z)} dz.$$

4.2. An approximation lemma.

Lemma 2. *Let $f : I \rightarrow \mathbb{C}$ an integrable function, of bounded variation, and supported on $I^\circ = (-1/2, 1/2)$. For $N \geq 2$, let*

$$f * |\mathbf{D}_N|^2(x) = \int_I f(y) |\mathbf{D}_N(x - y)|^2 dy, \quad x \in I.$$

Then

$$(4.2) \quad \left\| f - \frac{1}{N} f * |\mathbf{D}_N|^2 \right\|_{L^1(I)} \lesssim \text{Var}(f, I) \frac{\log N}{N}.$$

Remark 1. *In the above estimate, $\text{Var}(f, I)$ denotes the total variation of f on I . If $f = 1_{[-W, W]}$, with $W \in (-1/2, 1/2)$, then $\text{Var}(f, I) = 2$ and the estimate reads*

$$\left\| 1_{[-W, W]} - \frac{1}{N} 1_{[-W, W]} * |\mathbf{D}_N|^2 \right\|_{L^1(I)} \lesssim \frac{\log N}{N}.$$

Proof. By an approximation argument, we assume without loss of generality that f is smooth (see for example [2, Lemma 3.2]). We also extend f periodically to \mathbb{R} . Note that this extension is still smooth because $f|I$ is supported on I° .

Step 1. Since $f(x + h) - f(x) = \int_0^1 f'(th + x)h dt$, we can use the periodicity of f to estimate

$$\begin{aligned} \|f(\cdot + h) - f\|_{L^1(I)} &\leq \int_0^1 \int_{-1/2}^{1/2} |f'(th + x)| dx |h| dt = \int_0^1 \int_{-1/2+th}^{1/2+th} |f'(x)| dx |h| dt \\ &= \int_0^1 \int_{-1/2}^{1/2} |f'(x)| dx |h| dt = \text{Var}(f, I) |h|. \end{aligned}$$

Since f is periodic, the previous estimate can be improved to:

$$(4.3) \quad \|f(\cdot + h) - f\|_{L^1(I)} \lesssim \text{Var}(f, I) |\sin(\pi h)|, \quad h \in \mathbb{R}.$$

Step 2. We use the notation $f^N := f * \frac{1}{N} |\mathbf{D}_N|^2$. By a change of variables and periodicity,

$$f(x) - f^N(x) = \frac{1}{N} \int_{-1/2}^{1/2} (f(x) - f(y + x)) |\mathbf{D}_N(-y)|^2 dy.$$

We can now finish the proof by resorting to (4.3):

$$\begin{aligned} \|f - f^N\|_{L^1(I)} &\lesssim \text{Var}(f, I) \frac{1}{N} \int_{-1/2}^{1/2} |\sin(\pi y)| |\mathbf{D}_N(y)|^2 dy \\ &\lesssim \text{Var}(f, I) \frac{1}{N} \int_0^{1/2} \frac{|\sin(\pi N y)|}{|y|} dy \\ &\lesssim \text{Var}(f, I) \frac{1}{N} \left[1 + \int_1^{N/2} \frac{1}{|y|} dy \right] \\ &\lesssim \text{Var}(f, I) \frac{\log N}{N}. \end{aligned}$$

□

4.3. Proof of Lemma 1. We first note from (4.1) that

$$(4.4) \quad \text{trace} (H_W^N) = \int_I K_W^N(x, x) dx = \int_{[-W, W]} \int_I |\mathbf{D}_N(x - y)|^2 dy dx = 2NW,$$

since $\int_I |\mathbf{D}_N|^2 = N$. Moreover a similar calculation gives

$$\text{trace} (H_W^N)^2 = \int_{[-W, W]} \int_I \mathbf{1}_{[-w, w]}(y) |\mathbf{D}_N(x - y)|^2 dy dx.$$

Hence we can use Lemma 2 to conclude that

$$\begin{aligned} \text{trace} \left[(H_W^N) - (H_W^N)^2 \right] &= \int_{-W}^W \left[N \mathbf{1}_{[-w, w]}(x) - \left(\mathbf{1}_{[-w, w]} * |\mathbf{D}_N|^2 \right)(x) \right] dx \\ &\leq \int_I \left| N \mathbf{1}_{[-w, w]}(x) - \left(\mathbf{1}_{[-w, w]} * |\mathbf{D}_N|^2 \right)(x) \right| dx \leq C \log N, \end{aligned}$$

for some constant C . Using this bound, we estimate:

$$\begin{aligned} C \log N &\geq \sum_{k=0}^{N-1} \lambda_k (1 - \lambda_k) = \sum_{k=0}^{K-1} \lambda_k (1 - \lambda_k) + \sum_{k=K}^{N-1} \lambda_k (1 - \lambda_k) \\ &\geq \lambda_{K-1} \sum_{k=0}^{K-1} (1 - \lambda_k) + (1 - \lambda_{K-1}) \sum_{k=K}^{N-1} \lambda_k \\ &= \lambda_{K-1} K - \lambda_{K-1} \sum_{k=0}^{K-1} \lambda_k + (1 - \lambda_{K-1}) (2NW - \sum_{k=0}^{K-1} \lambda_k) \\ &= \lambda_{K-1} K + 2NW (1 - \lambda_{K-1}) - \sum_{k=0}^{K-1} \lambda_k \\ &= 2NW - \sum_{k=0}^{K-1} \lambda_k + \lambda_{K-1} (K - 2NW) \\ &\geq K - \sum_{k=0}^{K-1} \lambda_k - 1. \end{aligned}$$

Hence, $K - \sum_{k=0}^{K-1} \lambda_k \leq C \log N + 1$. On the other hand $\sum_{k=0}^{K-1} \lambda_k - K \leq 2NW - K \leq 1$. Therefore, since $N \geq 2$, $\left| K - \sum_{k=0}^{K-1} \lambda_k \right| \lesssim \log N$ and the conclusion follows.

REFERENCES

- [1] L. D. Abreu, A. S. Bandeira, *Landau's necessary density conditions for the Hankel transform*, J. Funct. Anal. 162 (2012), 1845-1866.
- [2] L. D. Abreu, K. Gröchenig, J. L. Romero, *On accumulated spectrograms*, Trans. Amer. Math. Soc., 368 (2016), 3629-3649.

- [3] M. Bayram, R. G. Baraniuk *Multiple window time-varying spectrum estimation*, In Nonlinear and Non-stationary Signal Processing (Cambridge, 1998), pages 292-316. Cambridge Univ. Press, Cambridge, 2000.
- [4] J. J. Benedetto, *Harmonic analysis and spectral estimation*, J. Math. Anal. Appl., **91** (1983), 444-509.
- [5] G. Bond, W. Showers, M. Cheseby, R. Lotti, P. Almasi, P. deMenocal, P. Priore, H. Cullen, I. Hajdas, G. Bonani, *A Pervasive Millennial-Scale Cycle in North Atlantic Holocene and Glacial Climates*, Science (1997), **278**, 1257-1266.
- [6] F. A. Dahlen, F. J. Simons, *Spectral estimation on a sphere in geophysics and cosmology*, Geophys. J. Int. (2008) **174**, 774-807.
- [7] A. Delorme, S. Makeig, *EEGLAB: an open source toolbox for analysis of single-trial EEG dynamics including independent component analysis* - J. Neurosci. Methods, (2004) **134**, 9-21.
- [8] S. Haykin, D. J. Thomson, J. H. Reed, *Spectrum sensing for cognitive radio*, Proc. IEEE, (2009), **97**, 849 - 877.
- [9] C. Harig, F. J. Simons, *Mapping Greenland's mass loss in space and time*, Proc. Natl. Acad. Sci. USA, (2012), **109**, 19934–19937.
- [10] S. Haykin, *Cognitive radio: brain-empowered wireless communications*, IEEE Journal on Selected Areas in Communications, **23** (2), 201-220, 2005.
- [11] J. A. Hogan, J. D. Lakey, *Duration and Bandwidth Limiting. Prolate Functions, Sampling, and Applications*, Applied and Numerical Harmonic Analysis, Birkhäuser/Springer, New York, 2012, xvii+258pp.
- [12] H. J. Landau. Sampling, data transmission, and the Nyquist rate. *Proc. IEEE*, 55(10):1701–1706, October 1967.
- [13] H. J. Landau. On Szegő's eigenvalue distribution theorem and non-Hermitian kernels. *J. Anal. Math.*, 28:335–357, 1975.
- [14] H. J. Landau and H. O. Pollak. Prolate spheroidal wave functions, Fourier analysis and uncertainty II. *Bell System Tech. J.*, 40:65–84, 1961.
- [15] K. S. Lii and M. Rosenblatt, Prolate spheroidal spectral estimates. *Stat. Probab. Lett.*, 78 (11), 1339-1348, 2008.
- [16] S. C. Olhede, A. T. Walden, *Generalized Morse wavelets*, IEEE Trans. Signal Process, 50 (11), 2661-2670, 2002.
- [17] D. B. Percival, A. T. Walden, *Spectral Analysis for Physical Applications, Multitaper and Conventional Univariate Techniques*. Cambridge, 1993, Cambridge University Press.
- [18] A. Plattner, F. J. Simons, *Spatiospectral concentration of vector fields on a sphere*, Appl. Comp. Harm. Anal. 36 (1), (2014) 1-22.
- [19] F. J. Simons, F. A. Dahlen, and M. A. Wiecezorek. Spatiospectral concentration on a sphere. *SIAM Rev.*, 48(3):504–536 (electronic), 2006.
- [20] D. Slepian, *Some comments on Fourier analysis, uncertainty and modeling*, SIAM Rev. **25** (1983) 379-393.
- [21] D. Slepian, *Prolate spheroidal wave functions, Fourier analysis and uncertainty-IV: Extensions to many dimensions; generalized prolate spheroidal functions* Bell Syst. Tech. J., (1964), 3009-3057.
- [22] D. Slepian and H. O. Pollak. Prolate Spheroidal Wave Functions, Fourier Analysis and Uncertainty I. *I. Bell Syst. Tech. J.*, 40(1):43–63, 1961.
- [23] D. J. Thomson, *Spectrum estimation and harmonic analysis*, Proc. IEEE, **70**, (1982) 1055-1095.

- [24] D. J. Thomson, *Multitaper Analysis of Nonstationary and Nonlinear Time Series Data*, Nonlinear and Nonstationary Signal Processing, Cambridge University Press, (2000).
- [25] A. T. Walden, E. J. McCoy, D. B. Percival, *The variance of multitaper spectrum estimates for real Gaussian processes*. IEEE Trans. Signal Process, **42** (1994), 479-482.
- [26] Z. Zhao, A. Singer, *Fourier-Bessel Rotational Invariant Eigenimages*, The Journal of the Optical Society of America A, 30 (5), pp. 871–877 (2013).

ACOUSTICS RESEARCH INSTITUTE, AUSTRIAN ACADEMY OF SCIENCE, WOHLLEBENGASSE 12-14 A-1040, VIENNA AUSTRIA

E-mail address: labreu@kfs.oeaw.ac.at

FACULTY OF MATHEMATICS, UNIVERSITY OF VIENNA, OSKAR-MORGENSTERN-PLATZ 1, A-1090 VIENNA, AUSTRIA

E-mail address: jose.luis.romero@univie.ac.at